

SYNTHESIS OF ZNO NANOFLOWERS AND THEIR WETTABILITIES AND PHOTOCATALYTIC PROPERTIES

X.D. Guo¹, L. E. Heleseth¹, Q.Z. Zhao²

¹ Department of Physics and Technology, University of Bergen, Allégaten 55, 5007 Bergen, Norway

² State Key Laboratory of High Field Laser Physics, Shanghai Institute of Optics and Fine Mechanics, Chinese Academy of Sciences, Shanghai 201800, China

Abstract — By employing hydrothermal growth, we demonstrate the growth of three-dimensional flowerlike ZnO nanostructures from aqueous solution. Our approach offers synthetic flexibility in controlling film architecture, coating texture and crystallite size. The wettability is studied by measurement of time-dependent contact angles in the as-grown samples. In addition, superior photocatalytic activity of the flowerlike ZnO nanostructures in the degradation of Rhodamine B is investigated as well. The influence factors and formation mechanism of the flowerlike ZnO nanostructures are also analyzed and discussed.

Keywords : Zinc Oxide, Hydrothermal Growth, Laser Direct Writing

I - Introduction

In the past decades, ordered nanostructures with controlled surface area and crystal morphologies have attracted great interest because the morphology of most nanostructures can effectively tune their intrinsic chemical and physical properties. Extensive work has been devoted to synthesize one-dimensional (1D) nanostructures and two-dimensional (2D) nanostructures such as nanoparticles, -wires, -belts, -tubes, -rings, -springs, -bows, -combs, -disks, etc [1-3]. Compared to 1D and 2D nanostructures, complex 3D architectures may offer opportunities to explore novel properties of nanocrystals and be employed as novel building blocks to fabricate more complicated and advanced materials. Up to now, various vapor methods such as thermal evaporation [4], chemical vapor deposition [5], vapor-liquid-solid (VLS) assisted [6], have been developed to prepare oriented nanostructures, but these methods typically require high temperatures and vacuum conditions, which limit the choice of substrate and the economic viability of high-volume production. In comparison with traditional vapor deposition approaches, the mild hydrothermal process using thermal treatment of the reactants may be the simplest and most effective way to prepare highly crystalline products at low temperatures. Moreover, this method allows considerable influence of reaction species on the final size and morphology of the as-synthesized samples on a large scale.

To fabricate nanostructures in the desired position, researchers have demonstrated a few techniques base on an assembly method under the control of external forces. Xu et al. have reported a technique of growing

vertically aligned ZnO nanowire (NW) arrays on a silicon substrate coated with ZnO seeds by electron beam lithography [7]. Aizenberg investigated the combination of self-assembled monolayers (SAMs) and micro contract printing to prepare spatially controlled micropatterns of calcite crystals on surface with controlled location [8]. Zhou et al. have reported a selective growth of ZnO nanorods arrays by using proton beam writing [9]. Kim has presented an approach for the preparation of ZnO nanowire arrays by combining laser-interference lithography for templating and a chemical-vapor-transport process for nanowire growth [10].

In this paper, we report the growth of 3D flowerlike ZnO nanostructures on GaN/LiAlO₂ by combing laser direct writing and hydrothermal method. In contrast with some flowerlike structures which formed by self-assembly technologies using nanoparticles, nanorods, and nanobelts as building blocks, the structures present here show uniform 3D structured flowers with nanosheets-constructed network morphology. Several parameters including both hydrothermal growth conditions and laser irradiation were present. A possible mechanism that may illustrate the flowerlike nanostructures formation is discussed. The 3D flowerlike ZnO nanostructures reported here could be important for applications in the transistor, optoelectronics, field emission, and gas sensing.

II - Experimental Details

Figure 1 shows the schematic diagram of the selective growth of ZnO nanostructures on the GaN/LiAlO₂ substrate. The process mainly involved three steps.

Substrate preparation. The GaN/LiAlO₂ substrate was prepared by depositing about 2.0 μm thick GaN film on LiAlO₂ with low temperature GaN buffer layers by metal-organic chemical vapor deposition (MOCVD). The as-prepared substrate was cleaned by a standard cleaning progress, and then a 1-μm-thick layer of PMMA (polymethyl methacrylate) was spin coated on the substrate at a rotation speed of 4000 rotation per minute. After that, the substrate was baked on a hot plate at 100°C for 2 min.

Laser direct writing. Micropatterning of the as-prepared substrate was conducted by a femtosecond laser system. A commercial regenerative amplified Ti:Sapphire laser (RegA 9000, Coherent) that emits polarized light with pulse duration of 150 fs and a repetition rate of 1 KHz was used in this experiment. The sample

was mounted on a computer-controlled xyz translation stage. The surface of the sample was positioned perpendicular to the propagation direction of the incident laser beam in the focal plane of a 100 \times objective lens (NA=0.8). The number of pulses delivered to the sample is controlled via an electromechanical shutter, and the laser pulse energy was measured by a pyroelectric detector.

Hydrothermal Growth. The nutrient solution was prepared from an aqueous solution containing zinc nitrate [Zn(NO₃)₂ · 6H₂O] and hexamethyltetramine [(CH₂)₆N₄, HMT] at a molar ratio of 1:1 and zinc concentration of 0.025 mol/L. Subsequently, the substrates were immersed downward into the reaction solution and heated at a constant temperature of 90 $^{\circ}$ C in a water bath for 1h with continue stirring. After deposition, the substrate was thoroughly washed with deionized water and dried in air at room temperature.

The morphology and composition of the as-prepared products were characterized by a field emission scanning electron microscopy (FE-SEM) (JEOL JSM-6700F) which was equipped with an energy-dispersive spectroscopy (EDS) facility. TEM images, SEAD pattern, and HRTEM images were taken on a JEOL-2010 transmission electron microscope.

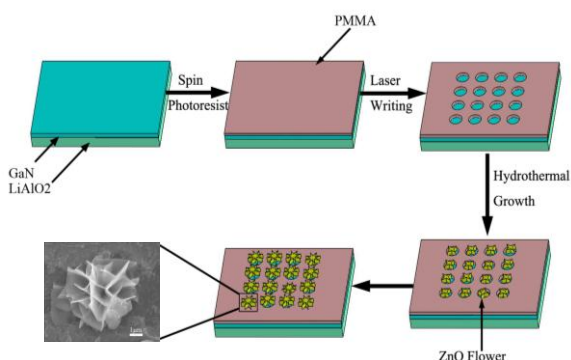


Figure1: Fabrication process of 3D flowerlike nanostructures: deposition of a PMMA layer on a GaN/LiAlO₂ substrate, laser processing and hydrothermal growth of ZnO nanostructure.

III - Results and Discussion

Figure 2a shows a typical SEM image of a single ZnO flower. It is clear to see that the diameter of the obtained flower was approximately 10 μ m and the flower consisted of 2D nanosheet. The number of pulses delivered to the sample is controlled via an electromechanical shutter. In this dot, the substrate was irradiated by 20 femtosecond laser pulses with energy of 1 μ J. There are some laser induced nanoripples appeared around the flower, this kind of structures have been discussed in our former papers [11]. Figure.2 (b) clearly demonstrates that by tuning the number of irradiated laser pulses as 250, 20 and 8, the ablated area can be adjusted and subsequent growth of ZnO flowers changed correspondingly. We successfully obtained

ZnO flowers with diameter of 10 μ m, 5 μ m, and 3 μ m, respectively. Controlling flower density is another important aspect in spatial organization; this can be achieved by the computer-controlled xyz translation stage. Figure 2 (c) shows a matrix of flowers, the distance between the flowers can be mediated through the pre-determined dots. What surprising us is that while the substrate was irradiated in line-scan mode, the flowers grow out of the opening could form corresponding long range architecture along the irradiated lines (figure.2 d). The as-grown ZnO flowerlike structures were prepared by the hydrothermal method which could introduce excess zinc or oxygen vacancies.

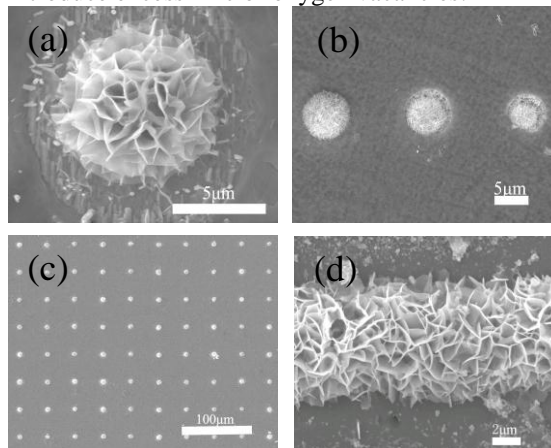


Figure2: SEM image of single flowerlike ZnO nanostructures, (b) SEM image of flowers with different size, (c) a matrix of flowers, (d) line-mode flowerlike nanostructure.

Higher magnification SEM images shown in figure 3(a) demonstrate the detailed structural information of the sample. We can find that the observed structure is constructed by many nanosheets with an average thickness of 100nm. Further insight into the morphology and microstructure of the flowerlike ZnO nanostructures were gained by using TEM and high-resolution TEM. Figure 3(b) presents a TEM image for a typical isolated ZnO nanosheet obtained by ultrasonic dispersion of the as-prepared sample in ethanol. Enlarged view of the rectangular area in panel a shows that each petal has a dense structure, the smooth surface consist of inter connected nanoparticles (figure 3c). The electron diffraction pattern (inset of figure 3c) recorded from the edge of the nanopetals displays several concentric diffraction rings and some regular diffraction spots, indicating the polycrystalline nature of the petals. The high-resolution TEM image exhibits well-resolved two-dimensional lattice fringes, as shown in figure 3(d). It can be concluded that the nanoparticles themselves are single-crystalline, whereas the whole hierarchical structures are polycrystalline due to the anisotropic assembly of the building blocks.

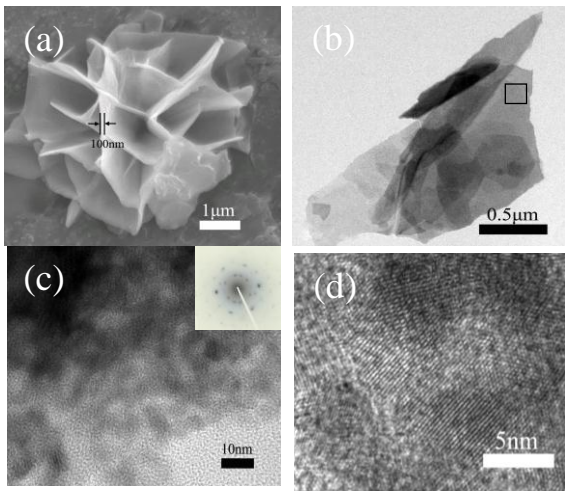


Figure 3: (a) SEM image of an individual ZnO flower. (b) TEM image of a typical nanosheet. (c) Enlarged view that corresponds to the small frame area marked in the nanosheet, the inset is the SAED pattern of the nanosheets. (d) High-resolution TEM image.

During the irradiation process, femtosecond laser pulse could generate a very dense electron-hole which could destabilize the lattice when a critical carrier concentration is exceeded. Because the duration of laser pulse is very short (150fs), the arrangement of crystal lattice is of short order, new bonds between the atoms could be formed. The accumulated laser pulse energy can be stored in the irradiated region in the form of crystallographic changes, such as re-crystallization-supported stress. In the hydrothermal growth, because the crystal habit was governed by the growth rates of different crystallographic facets, the negative nature of the growth unit will lead to different growth rates of planes, the interior strain in the irradiated dot could create distortion and dislocation in the orientation of the crystal planes.

To further understand the growth mechanism of the flowerlike ZnO nanostructures, systematical time-dependent experiments illustrating the evolution of the structure were carried out. When the reaction proceeds for 5 min, some sprouts grow out from the irradiated dot (figure 4a). When the reaction time extends to 10 min, the sprouts grow larger and formed some petals (figure 4b). After 30 min, a small flower is formed. When the reaction time is increased to 2h, the 3D flowerlike nanostructures appear, and almost no impurities can be observed. To determine the appropriate reaction time, the effect of longer reaction times, up to 12h, has been investigated. Results show that the reaction time exceeding 2h will not bring about evident structural and morphological modifications. With reaction time increasing, the concentration of ZnO nuclei decreases conversely, and the growth velocity of ZnO nanopetals decrease along with the reactant concentration. As a result, the morphology changes very little after a certain period.

The growth of ZnO flowerlike structures is controlled by nucleation and growth process in aqueous solution [12]. In the hydrothermal process, the negative

nature of the growth unit $[\text{Zn}(\text{OH})_4^{2-}]$ will lead to

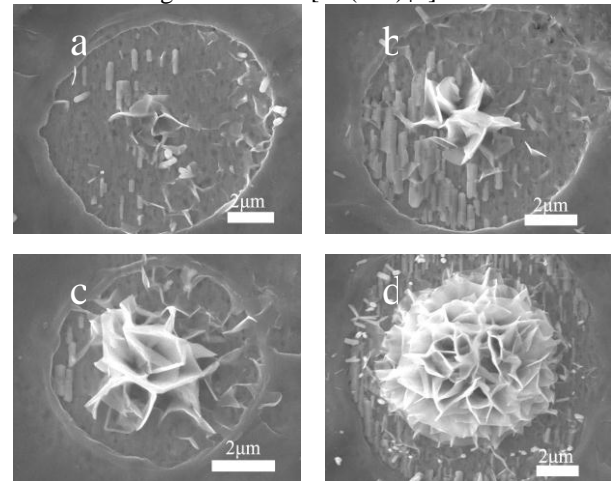


Figure 4: SEM images of the samples at different times after the temperature reached 90 °C: (a) 5, (b) 10, (c) 30, (d) 120 min, respectively.

different growth rates of planes, when there is no organic additive in solution, spherical ZnO particles will be easily developed because of the Ostwald ripening process. In our experiments, HMT is expected to serve as the organic template during the heating process to 90 °C, thus dynamically modifying the nucleation process. The substrate/crystal surface has a boundary layer of charged ions, the thickness of which is diffusion controlled. With the concentrations of Zn^{2+} and OH^- increase, $\text{Zn}(\text{OH})_2$ and/or ZnO nuclei will be developed under the low precursor concentration and the action of HMT. In some studies, the formation of ZnO sheets and plates has been attributed to a 1D branching and subsequent 2D interspaces filling process to give a final 3D structure. In the present case, the nanosheet might be the result of the self-assembly of a number of active sites that trigger the nucleation at the interface, promoting the formation of petal crystals extending from the interface.

It is well known that the wettability of a solid surface is closely related to its micro/nanostructures, because structure or texture could influence the spreading of liquids. In our experiment, the time-dependent water CA measurements were conducted on the ZnO grid surfaces. The water CA of ZnO grid in our experiments changed from 92° at the beginning to almost 0° after 40 minutes, the droplet evaporation time is about 60 min. During the measurement, the out most edge of the droplet is fixed. The CA varies as a function of time is expressed as $\theta = \theta_i (1 - t/t_f)$, where θ_i is the initial contact angle and t_f is the total evaporation time [13]. In our experiments, we can see that some changes occur on the surrounding region of the water droplet from the CCD images. It is reasonable to conclude that the liquid penetrated the interstitial spaces between the features, leading to the rapid decrease of contact angle.

The study of photocatalytic activities is important for searching strategies to design functional nanostructures. The as-produced ZnO nanoflowers were investigated for the applicability in photodegrading organic dyes of Rhodamine B (RB). The use of this aromatic

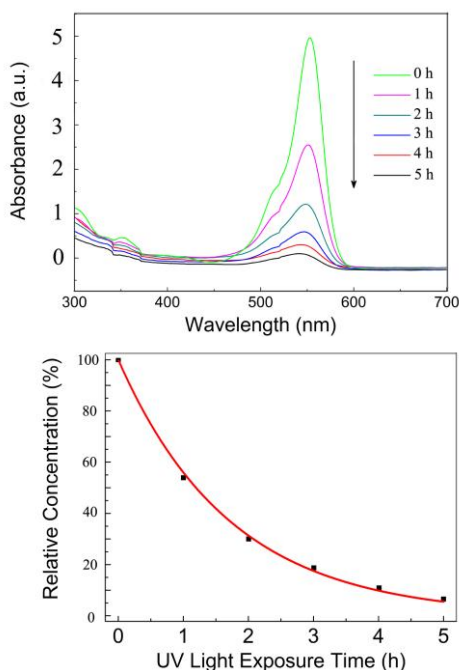


Figure 5: (a) UV-vis adsorption spectra of MB solution catalyzed by the ZnO nanostructure films under UV irradiation. (b) Degradation of the MB under UV irradiation as a function of time.

compound as a model dye is mainly due to their recurrent occurrence in the industrial field. The reaction time was scheduled to be 0, 1, 2, 3, 4 and 5 h, respectively. The degradation is monitored by studying the decrease in absorbance of RB and quantified by plotting a first order decay plot of the absorbance. As shown in Figure 5a, the absorption spectra corresponding to the RB molecules at 552 nm decreases in intensity rapidly with the extension of exposure time. The decomposition rate is high within the first 2 h. With time evolution, the concentration of RB decreases, the probability of RB reacting with ZnO nanostructures decreases, and consequently, the decomposition rate decreases.

The photodegradation of RB solution accords with the exponential decay formula $C(t)=C(0)\exp(-kt)$, [14] where $C(t)$ is the relative concentration of RB at time t , $C(0)$ is the initial relative concentration, and k is the photodegradation rate constant, the result is plotted and shown in Fig. 3b. The solid squares are the experimental data, and the solid line is the fitting curve. The rate constant of the degradation reaction for RB is $0.58 \pm 0.03 \text{ h}^{-1}$. It is worth to mention that, due to the very small thickness and low density of the nanostructures on the substrate, the total weight of the nanostructures that evolved in the photodegradation is less than 0.1 mg, which cannot be determined by our analytical balance. Further experiments required to clarify the relationship between the weight of the nanostructures and the degradation rate, and to compare it with normal photocatalysts in degradation of organic dyes.

IV - Conclusion

We have demonstrated the fabrication of 3D flower-like ZnO nanostructures by combining laser direct writing and hydrothermal growth method. The control of the as-fabricated ZnO flowerlike structures can be achieved by altering hydrothermal growth conditions as well as laser irradiation parameters. Possible mechanisms for the formation of different nanostructures have been proposed. We expect that the methodology for controlling the shape of ZnO nanocrystals demonstrated in this work could provide a great opportunity to fully explore their application in the field of fabrication of nano-electronic devices.

References

- [1] Z.S. Hu, J.E. Ramirez, B.E. Cervera, G. Oskam and P. C. Searson, *J. Phys. Chem. B* vol. 109, PP. 11209-11214, 2005.
- [2] M.H.Huang, Y. Wu, H. Feick, N. Tran, E. Weber and P. Yang, *Adv. Mater.* vol.13, pp.113-116, 2001.
- [3] Z.W. Pan, Z.R. Dai and Z.L. Wang, *Science* 291, pp. 1947-1949, 2001.
- [4] G.Z. Shen, J.H. Cho and C.J. Lee, *Chem. Phys. Lett.* vol. 401, pp. 529-533, 2005.
- [5] S. Muthukumar, C.R. Gorla, N.W. Emanetoglu, S. Liang and Y.J. Lu, *J. Cryst. Growth*, vol. 225, pp. 197-201, 2001.
- [6] C. J. Barrelet, Y. Wu, D.C. Bell and C.M. Lieber, *J. Am. Chem. Soc.* vol. 125, pp. 11498-11499, 2003.
- [7] S. Xu, Y. Ding, Y.G. Wei, H. Fang, Y. Shen, A.K. Sood, D.L. Polla and Z.L. Wang, *J. Am. Chem. Soc.* vol. 130, pp. 14958-14959, 2008
- [8] Aizenberg, J. *Adv. Mater.* vol. 16 pp. 1295-1302, 2004.
- [9] H.L. Zhou, P.G. Shao, S.J. Chua, J.A. Kan, A.A. Bettiol, T. Osipowicz, K.F. Ooi, G. Goh and F. Watt, *Cryst. Growth Des.* vol. 8 pp. 4445-4448, 2008.
- [10] D.S. Kim, R. Ji, H.J.Fan, F. Bertram, R. Scholz, A. Dadgar, K. Nielsch, A. Krost, J. Christen, U. Gosele and M. Zacharias, *Small* vol. 3 pp. 76-80, 2007.
- [11] X. D. Guo, R. X. Li, Y. Hang, Z.Z. Xu, B.K. Yu, Y. Dai, B. Lu and X.W. Sun, *Appl. Phys. A* vol. 94, pp. 423-426, 2009
- [12] F. Xu, Y.N. Lu, Y. Xie and Y.F. Liu, *J. Phys. Chem. C* vol. 113, pp.1052-1059, 2009.
- [13] J.H. Park, H.J. Choi, Y.J. Choi, S.H. Sohn and J.G. Park, *J. Mater. Chem.* vol. 14, pp.35-36, 2004.
- [14] J. Matos, J. Laine, and J. M. Hermann, *Appl. Catal. B: Environ.* vol. 18 (3-4), pp. 281-291, 1998.